HAL
open science

Modelling and Control Structure of a Phosphorite Sinter Process with Grey System Theory

Nigina Toktassynova, Hassen Fourati, Batyrbek Suleimenov

To cite this version:

Nigina Toktassynova, Hassen Fourati, Batyrbek Suleimenov. Modelling and Control Structure of a Phosphorite Sinter Process with Grey System Theory. The Journal of Grey System, 2020, 32 (2), pp.150-166. hal-02967808

HAL Id: hal-02967808

https://inria.hal.science/hal-02967808

Submitted on 15 Oct 2020

HAL is a multi-disciplinary open access archive for the deposit and dissemination of scientific research documents, whether they are published or not. The documents may come from teaching and research institutions in France or abroad, or from public or private research centers.

L'archive ouverte pluridisciplinaire **HAL**, est destinée au dépôt et à la diffusion de documents scientifiques de niveau recherche, publiés ou non, émanant des établissements d'enseignement et de recherche français ou étrangers, des laboratoires publics ou privés.

Modelling and Control Structure of a Phosphorite Sinter Process with Grey System Theory

Nigina Toktassynova[1*], Hassen Fourati[2], Batyrbek Suleimenov[1]

1. Department of Automation and Control, Satbayev University, Almaty 050013, Kazakhstan
2. Univ. Grenoble Alpes, CNRS, Inria, Grenoble INP (Institute of Engineering Univ. Grenoble Alpes), GIPSA-Lab, Grenoble 38000, France

Abstract
The sintering process of phosphorite ore occurs with a large amount of return caused by untimely process control. The control task of the phosphorite ore sintering is to regulate parameters of the process to obtain a high-quality sinter. The parameter clearly responsible for the sinter quality is the temperature in the wind box (also called burn through point (BTP)). Therefore, in order to solve the real-time control task, it is necessary to predict the BTP. In this paper, the grey system theory is used as a predictive approach, which makes it possible to obtain an adequate model that has the character of a "generalized energy system" and uses a small initial sample. Based on the grey model GMC(1,n), which is constructed in real-time by using real data at the beginning of the process, the temperature is well predicted at the end of the sintering process. When the temperature does not match the set value or to find out an optimal regulation, a control synthesis is carried out through an optimization of the prediction according to the "particle swarm" algorithm.

Keywords: Grey System; Sintering Process; Particle Swarm Optimization; Predictive Model; Prediction Optimization

1. Introduction
Sintering in metallurgy is a thermal process that occurs in a metallurgical charge, composed of ore pellets, concentrates, and fuel (coke). Due to the process non-linearity, the real-time quality control is a complicated task. In practice, the operator makes changes to the process after the product is obtained, which leads to a large number of returns and expenses for re-sintering. In this regard, it becomes necessary to predict sinter quality in advance and control the process based on predictive data. One of the key indicators of the sintering quality is the burn through point (BTP) that indicates the sintering process completion and represents the point with the highest temperature. The problem of BTP prediction and control is studied in many works using various algorithms such as neural networks, genetic algorithms, cluster analysis, and fuzzy control. Due to the evolution and widespread use of neural networks, a large number of works related to prediction, use this method in various fields of research such as the BTP prediction and control. For example in the work[1], a new predictive parameter (the mathematics inflexion point of waste gas temperature curve in the middle of the strand) was measured at different times (600

[*]***Corresponding Author:*** *Toktassynova Nigina, Department of Automation and Control, Satbayev University, Almaty 050013, Kazakhstan; Email: tamaki1992@gmail.com*

groups of data) and fed to the input of a multilayer neural network, whose output predicts the BTP values by 5 steps forward. The neural network is also used in the work[2], where strand speed and BTP at the previous instants of time were given to the network inputs. The network, together with the training algorithm, was used to update the BTP model and called the neural network identifier, which used in the adaptive pole placement algorithm as an accurate model. In the work[3] the current value of BTP, temperatures in the middle, at the end of the process, and the strand speed were given to the input of a neural network to predict the BTP and make an intelligent control of the iron ore sintering process.

Some works use 2 BTP predictive models: temporary and technological. So to predict the permeability of lead-zinc ore in work[4] the temporary neural network was supplied with 6 previous values for permeability, and the technological neural network used the temperature of the fire, the humidity, the sulfur, lead, silicon dioxide content, and the strand speed. In the work[5] as a time sequence model, the grey model GM(1,1) of BTP of lead-zinc ore was applied, and parameters of the charge permeability and the strand speed of the pallets were fed to the technological neural network input. The the work[6] for BTP prediction of iron ore sintering also used the integration of grey model and neural networks. Here the result of the grey model GM(1,1), especially the gas temperature in wind boxes, is one of the inputs of the backpropagation neural network, along with the strand speed and the BTP at the current time. All three considered works with two predictive models used a fuzzy expert controller that maintains the BTP desired position within the specified boundaries.

In addition to standard learning algorithms for neural networks, genetic algorithms are used to optimize weights values. Thus, in the work[7] dedicated to the BTP control of iron ore sintering process, an adaptive genetic algorithm was used, where the input layer of the neural network is parameters of the initial material, density, strand speed, and ignition temperature, and the output layer is responsible for the values of temperature and pressure of sintering gases and gases in wind boxes. The genetic neural network was also used for the BTP prediction of iron ore sintering in the paper[8], where 707 groups of data were given to the input after clustering and classification of temperature and pressure vectors from 18 wind boxes. The system of adaptive structural clustering in this work used methods of spatial clustering of initial data, a self-organizing neural network map for extracting data relevancy properties, and a Kohonen map for learning network. The idea of clustering was used in the work[9] for the BTP prediction model of iron ore sintering. The K-means clustering module, whose inputs are the cold-charge permeability model, the ignition temperature, and the coke residue values, were used to form clusters. The predictive model in this paper did not use neural network algorithms. The clusters from the K-means module were fed to the dynamic model of temperature and vacuum. The dynamic model was constructed using the novel genetic programming. A firework algorithm based on a genetic algorithm was proposed in [10] to optimize the sintering terminal prediction model of the support vector machine. Seven main parameters were used as input to predict the BTP.

Models that do not use the neural networks for BTP prediction are based on equations of temperature or burn through time. Thus, for example, in the work[11] predicted value of the burn through time was determined by the least-squares method based on the historical data and, depending on the signal of the event-based model which determines the time until the end of the movement, the control of strand speed is carried out. The event-based model for the BTP of iron ore sintering is represented

by a linear time-constant discrete model in the state space, using the idea of breaking a continuous model into discrete events. In the work[12], a parabolic model was used to change the control temperature of BTP, compiled from the measured values in three wind boxes. It was used to determine and correct the volume of sintering gases, calculated from the volume of oxygen, humidity, and composition data of the charge. The work[13] describes a two-level hierarchical control system (intelligent control and automation level) of BTP and the vertical sintering rate of the iron ore sintering process, where the BTP model represents a piecewise-quadratic temperature depends on the strand position. In the work[14], a BTP control of iron ore sintering is divided into 2 parts: a closed-loop identification model and a generalized predictive control model. In the first part, the BTP is found based on the dynamic autoregressive exogenous model to calculate which strand speed, amount of moisture, the height of the charge, air volume, and vacuum is used. The closed-system identification method was used to determine the model parameters dynamically. In the second part, based on the transfer function obtained from the identification model, the BTP prediction was made to control the strand speed.

The state of BTP also was predicted using a particle swarm optimization algorithm (PSO) [15], where the degree of four influence parameters: suction pressure, air input, velocity of sintering machine, and ignition temperature, is found by PSO. According to the literature, we can conclude that: (1) prediction of BTP based on different parameters: data of vertical sintering rate, vacuum, permeability, the height of the charge, the temperature in wind boxes or sintering gases, strand speed, previous values of BTP; (2) high accuracy of the predictive model is achieved by using a large initial sample or historical data; (3) control of BTP is carried out by influence on strand speed.

However, in practice, due to lack of automation, only the main process parameters are often measured, such as temperature in wind boxes, vacuum, strand speed, charge height and mass values of the main components. The values of such properties as permeability, the volume of sintering gases, or properties of charge are obtained only by laboratory experiments. Therefore, it becomes necessary to construct a predictive model using the main measured parameters; in this work, we use the temperature in the wind boxes and vacuum. Obtaining a large sample of initial data is also difficult in production - it requires a long time to collect data and accumulate them to improve predictive accuracy. In this case, if certain conditions of the process (properties of the initial charge, charge height, pellet size, ignition gas, etc.) change, it will be necessary to collect data again and retrain the predictive model for obtaining accurate results. Therefore, it is necessary to use such a predictive model that will be adequate for training on a small initial sample and will be built in real-time. To solve this problem, the theory of grey systems developed by J. Deng in 1982 is used, which is focused on solving prediction problems with a small volume of the original sample and with poor information. The idea of the grey system theory is to consider the process as a “generalized energy system” and emphasize that non-negative smooth discrete functions can be transformed into a sequence having the approximate exponential law, which is the so-called grey exponential law[16]. The application of grey models was considered in the works[5, 6] as a part of BTP prediction. In the considered studies, the GM(1,1) model was used, in which only the previous values of the predicted variable influence the subsequent prediction. The disadvantage of this approach is the lack of consideration of influencing factors.

Therefore, in this paper, an improved grey model, the convolution integral model GMC(1,n) is used[17], which allows us to take into account (n-1) influencing factors

on the prediction of the charge highest temperature. The BTP prediction is necessary for the sintering process control. Since the model takes into account not only temperature but also pressure in wind boxes, the control task can be organized by changing two variables, the strand speed (standard approach) and the pressure. Then, the proposed approach in this paper is intended to solve the problem of the phosphorite ore sintering process control and based on the optimization of the prediction model.

The paper is organized as follows. Section 2 gives a general description of the sintering process and presents the three samples of the main parameters, which are obtained in the workshop. Section 3 is devoted to the grey predictive models, the convolution model construction algorithm, and the way to find the minimum volume of the initial sample. Section 4 presents the structure of the sintering process control based on predictive optimization. Section 5 presents some concluding remarks.

2. Sintering process

The phosphorite ore sintering process is produced in the Novozhambul phosphorus plant, which is located in the south of Kazakhstan, near the Karatau phosphor field. It is the second most crucial process in the plant, after the production of yellow phosphorus, for which the sinter is a raw material. The technological process is shown in Figure 1. It begins with a primary blending of the charge with a cold and a secondary return, which is introduced into the charge without dosing and lead to significant changes of the fuel in the charge. Then, the charge is poured to the moving grate and ignited with the help of natural gas or CO_2, passing under the horn (Figure 2, a). Due to the vacuum created by wind boxes, the heat from the fuel combustion is transferred to the underlying layers, evenly sintering a layer of 260 mm high as the grate moves to the end of the 78 m long sinter machine (Figure 2, b). Further, the agglomerate is cooled and crushed, and the poorly sintered charge is sent to the beginning of the process.

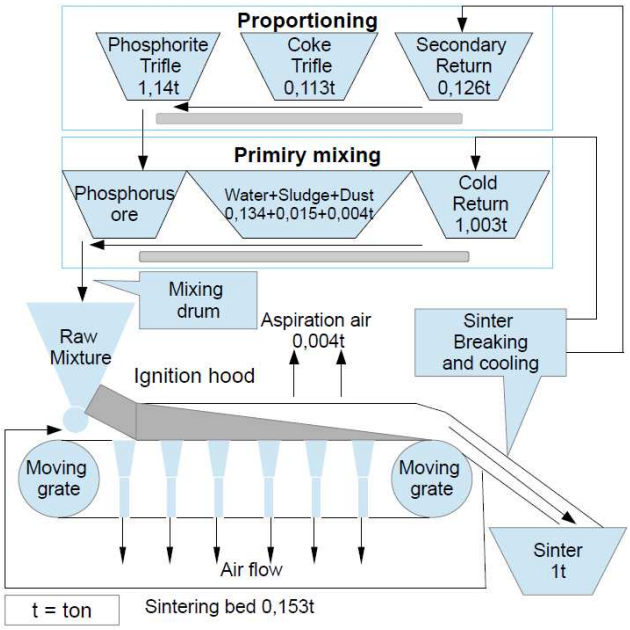

Figure 1 Technological chain of phosphorite ore sintering process

The amount of the sintering return reaches 40-50% since the process is controlled at the end of the sinter machine by an operator's decision based on the sinter slice. The amount of return needs to be reduced through a preliminary BTP prediction and control based on predictive data. The main parameter for the prediction is the temperature in the lower part of the strand (temperature in wind boxes). Temperature curves (Figure 3) are samples of data taken at different times, under different initial conditions: different charge composition, coke amount, pressure, but at the constant speed, so they are shown only until the desired temperature is reached in order to determine the duration of the process.

In addition, the pressure drop across the bed data Δp (the difference between the pressure in upper and lower parts of bed) is measured, and the gas velocity u (Figure 4) in the lower part of the charge is calculated using Ergun equation

$$\frac{\Delta p}{L} = \frac{150\mu u\left(1-\varepsilon\right)^2}{d^2\varepsilon^3} + \frac{1.75\rho u^2\left(1-\varepsilon\right)}{d\varepsilon^3} \tag{1}$$

where L is the height of the bed, $\mu\left[Pa.s\right]$ is the dynamic viscosity of gas, ε is the porosity of porous matrix, and $d\left[m\right]$ is the equivalent particle size. The porosity value is calculated according to the method proposed in [18].

(a) Under horn. (b) End of sintering machine.

Figure 2 Sintering machine in the Novozhambul phosphorus plant

To check whether the gas velocity affects the charge temperature, correlation methods are used, which reveals the statical relationship between the two variables. There exist a considerable number of correlation methods, such as Pearson's two-dimensional correlation, canonical, partial, point-biserial, Kendall's rank correlation, Spearman, and others. In this paper, the Spearman's rank correlation [-1;+1] is used, which is a non-parametric test and is used to measure the degree of association between two variables. The advantage of this method is that the distribution law of the original samples does not play a role. The calculation of the correlation can be found using the following function under Matlab – corr(x, y, Type, Spearman).

Also, due to the use of grey models in this work, Deng's grey relational analysis (GRA [0; 1]) is also executed as

$$r_j = \frac{1}{n}\sum_{k=1}^{n}\frac{\min_j\left|y\left(k\right)-x\left(k\right)\right| + \rho\max_j\left|y\left(k\right)-x\left(k\right)\right|}{\left|y\left(k\right)-x\left(k\right)\right| + \rho\max_j\left|y\left(k\right)-x\left(k\right)\right|} \tag{2}$$

where $\rho = 0.5$ is the *distinguishing coefficient*, which is used to increase the most prominent differences between two arrays x and y (x and y data are represented in

Appendix Table A1). One of the feature of GRA model, that it always reveals a positive correlation. Since Spearman's correlation coefficient is negative, it will be better to use the Bidirectional GRA model [26].

Algorithm of Bidiectional GRA model follows these steps:

1. Normalize the data sequences using the minimizing operator (normalized data in Appendix).
2. Generate the Mirror Sequences from normalized $\breve{x} = \left(x(n), x(n-1), \ldots, x(1)\right)$.
3. Calculate the Bidirectional Absolute Grey Relational Degrees

$$\varepsilon_{yx}^{\pm} = \begin{cases} +\max\left(\varepsilon_{yx}, \varepsilon_{y\breve{x}}\right), \varepsilon_{yx} - \varepsilon_{y\breve{x}} > 0 \\ -\max\left(\varepsilon_{yx}, \varepsilon_{y\breve{x}}\right), \varepsilon_{yx} - \varepsilon_{y\breve{x}} < 0 \end{cases}$$

where

$$\varepsilon_{yx} = \frac{1+|S_y|+|S_x|}{1+|S_y|+|S_x|+|S_y - S_x|},$$

$$|S_y| = \left|\sum_{k=2}^{n-1} y(k) + \frac{1}{2} y(n)\right|,$$

$$|S_x| = \left|\sum_{k=2}^{n-1} x(k) + \frac{1}{2} x(n)\right|, \text{ and}$$

$$|S_y - S_x| = \left|\sum_{k=2}^{n-1} \left(y(k) - x(k)\right) + \frac{1}{2}\left(y(n) - x(n)\right)\right|.$$

It can be seen from Table 1, for each sample the gas velocity must be taken into account to determine the charge temperature, since there is a strong relation between them close to $|1|$. Also, according to the Javed's Grey Incidence (JGI), scale $\varepsilon^{\pm} = [0.7; 0.8]$ is a third level of the strength of association between the sequences and means appropriately strong relation.

Table 1 Correlation results between temperature and gas velocity

Correlation type	Sample 1	Sample 2	Sample 3
Spearman	-0.4072	-0.7715	-0.7430
GRA	0.6690	0.6757	0.6839
Bidirectional GRA	-0.7485	-0.7509	-0.7589

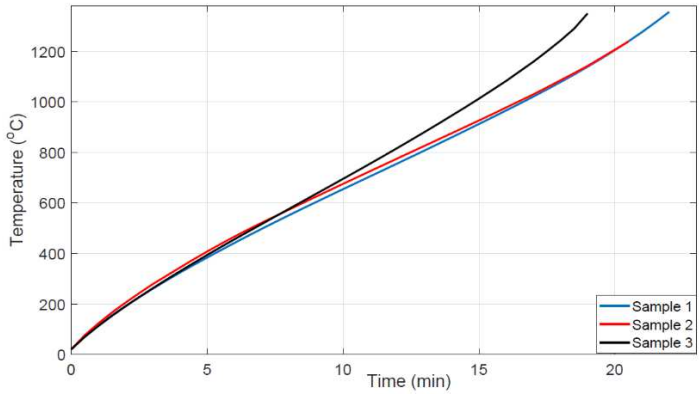

Figure 3 Temperature curves of 3 samples in wind boxes

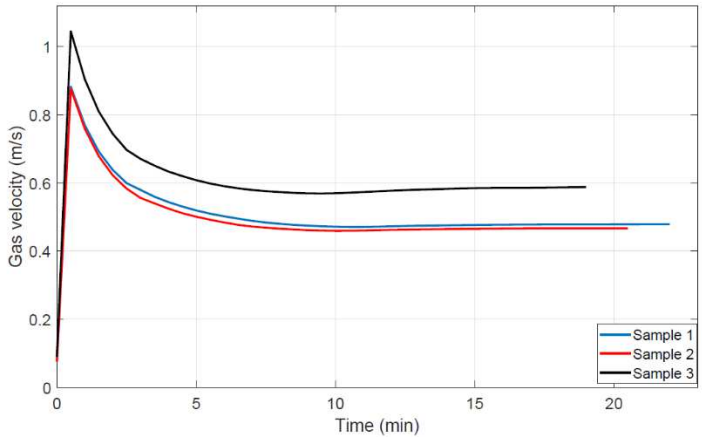

Figure 4 Gas velocity of 3 samples

3. Grey model approach

The influence of several factors on the predicted value for grey models can be considered only on the basis of model modifications GM(1,n), which is clearly demonstrated in the work[19]. A continuous convolution integral grey model GMC(1,n)[17] is one of the basic models with (n-1) influencing factors. On the basis of this model, other continuous linear grey models with (n-1) influencing factors were developed. For example, an interval model with a convolution integral IGDMC(1,n)[20], is intended for prediction of the interval in which the variable is located. Model FGMC(1,n) [21] is developed on the basis of the idea of prediction independence from the first pair of initial sample data. The deterministic grey model with the convolution integral DGDMC(1,n)[22] distinguishes from GMC(1,n) by the estimation of first derivative and parameters: the first derivative is estimated numerically by the cubic curve of the spline and the parameters of the model, according to the scheme of deterministic convergence. The error in the strength prediction considered by Tien is 0.54% for FGMC(1,n), 1.25% for GMC(1,n), 1.85% for DGDMC(1,n) and 3% for IGDMC(1,n). Finally, GMC(1,n) is chosen as the predictive model, since FGMC(1,n) uses an arbitrary pair of numbers that should be inserted in the front of the original series; therefore the prediction error is depending on this chosen number that can be different for the various composition of charge and difficult to find out optimal one. All GMC(1,n) models [23, 24] are focused on optimizing the model coefficients, to improve the model accuracy.

3.1 Convolution integral grey model GMC(1,n)

The gas velocity, calculated from the known pressure Δp, which is measured in real-time was selected as an influencing factor. Convolution integral grey model GMC(1,n) [17] (where n=2) with one influencing factor is a linear differential model

$$\frac{dY^{(1)}(t)}{dt} + b_1 Y^{(1)}(t) = b_2 X^{(1)}(t) + u \tag{3}$$

GMC(1, n) (n=2) is represented by (3) in which $Y^{(0)}$ is the predicted series, $X^{(0)}$ is the associated series, b_1 and u are the developmental coefficient and the grey control parameter respectively, and b_2 is the associated coefficients corresponding to the associated series $X^{(0)}$.

$Y^{(1)}(t)$ and $X^{(1)}(t)$ are 1-AGO data

$$Y^{(1)}(t)=\sum_{l=1}^{t}Y^{(0)}(l) \tag{4}$$

$$X^{(1)}(t)=\sum_{l=1}^{t}X^{(0)}(l) \tag{5}$$

The grey derivative for the first-order AGO data in (1) is conventionally represented as

$$\frac{dY^{(1)}(t)}{dt}=\lim_{\Delta t\to\infty}\frac{Y^{(1)}(t+\Delta t)-Y^{(1)}(t)}{\Delta t}=Y^{(1)}(t+\Delta t)-Y^{(1)}(t) \tag{6}$$

when $\Delta t\to 1$.

The parameters of (3) are determined using the least squares method

$$\left[b_1,b_2,u\right]^T=\left(B^TB\right)^{-1}B^TY_R \tag{7}$$

where t changes from 1 to r which is the number of initial sample to construct the model in (1).

$$B=\begin{bmatrix} -0.5\left(Y^{(1)}(1)+Y^{(1)}(2)\right) & 0.5\left(X^{(1)}(1)+X^{(1)}(2)\right) & 1 \\ -0.5\left(Y^{(1)}(2)+Y^{(1)}(3)\right) & 0.5\left(X^{(1)}(2)+X^{(1)}(3)\right) & 1 \\ . & . & . \\ . & . & . \\ . & . & . \\ -0.5\left(Y^{(1)}(r-1)+Y^{(1)}(r)\right) & 0.5\left(X^{(1)}(r-1)+X^{(1)}(r)\right) & 1 \end{bmatrix} \tag{8}$$

$$Y_R=\left[Y^{(1)}(2),Y^{(1)}(3),...,Y^{(1)}(r)\right]^T$$

Prediction of the sinter temperature $\hat{Y}^{(0)}(0-initial\ data)$ is determined by the following equation

$$\hat{Y}^{(0)}(t)=\hat{Y}^{(1)}(t)-\hat{Y}^{(1)}(t-1) \tag{9}$$

$$\hat{Y}^{(1)}(t)=Y^{(0)}(1)e^{-b_1(t-1)}+\frac{1}{2}e^{-b_1(t-1)}\left(b_2X^{(1)}(t)+u\right)+\frac{1}{2}\left(b_2X^{(1)}(t)+u\right)+\sum_{i=2}^{t-1}e^{-b_1(t-l)}\left(b_2X^{(1)}(l)+u\right) \tag{10}$$

3.2 Size of initial sample to construct the model

The size of the initial sample for constructing a predictive model is also an important parameter, which leads to reduce the error in temperature prediction. Also, it allows us to define wind boxes, where thermocouples should be installed in the future and reduce their quantity for the economy. The main feature of the grey theory is its capability to use as few as *n+3* pairs of data by GMC(1,n) [17]. For each sample, the following experiments were performed: (1) based on the n-pair of series from the sample, the model was built, (2) based on the model, the prediction of the remaining values was made, (3) the prediction results were compared to the original samples and the Root Mean Squared Percentage Error (RMSPE) according to (11) was calculated.

$$RMSPE=\sqrt{\frac{1}{n}\sum_i\frac{\left(\hat{Y}_i-Y_i\right)^2}{Y_i^2}}.100\% \tag{11}$$

During the experiments, models were built for each sample ranging from 5 (from 2.5 min from the start of the sintering process) to 20 (to 10 min from the start of the sintering process) pair of series. The results of the predicted errors for each sample are presented in Figure 5 (results from 2.5 to 5 min are omitted due to the large value of the predicted error). The predicted errors for each sample take the minimum values for different pairs of series, ranging from 14 (7 min) to 17 (8.5 min) pair of series. The mean smallest predictive error for 3 samples is achieved with 15 pairs of series (7.5 min).

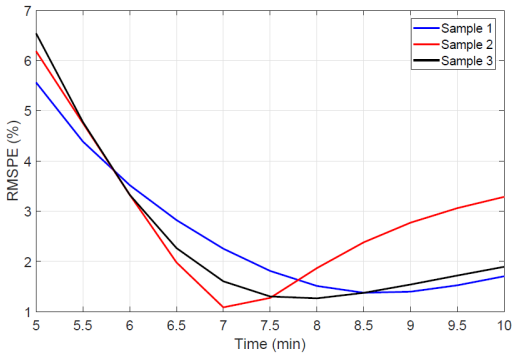

Figure 5 Predictive errors depending on different sample sizes

GMC(1,n) predictive models for 3 samples (Figure 3) are presented in Table 2, where the volume of initial sample r to construct the model includes data from the beginning of the sintering process up to 7.5 min (15 values). The parameters of the grey model, which were found by (7), differ significantly for each sample. This is due to the fact that each temperature curve was obtained under different initial conditions: the content of coke, phosphorite ore, the amount of return, moisture and other parameters of the charge, which are not directly taken to build a predictive model. Moreover, in production under real conditions, it is not possible to continuously control the composition of the charge, which makes it challenging to use a model that takes into account all the factors. Therefore, it is necessary to build a predictive model, which use only measured real-time factors and dynamically construct the predictive model for a certain batch of sintered ore. The results for the samples are shown in Figure 6 (data are provided in Appendix Table A2). Prediction error according to (11) for 3 samples, is shown in Table 2. The predictive results based on grey systems do not improve the accuracy in comparison with the other models, but allow to build an adequate prediction model of BTP in the absence of a large amount of historical temperature data. The additional advantage is the time saving for data collection and model training.

Table 2 GMC model of samples (n=2)

No. of sample	GMC(1,n)	RMSPE, %
1	$\frac{dY^{(1)}(t)}{dt} - 0.00176248Y^{(1)}(t) = 55.0012859X^{(1)}(t) + 41.90354212$	1.8115
2	$\frac{dY^{(1)}(t)}{dt} - 0.0030327Y^{(1)}(t) = 62.1579506X^{(1)}(t) + 41.27688268$	1.2746
3	$\frac{dY^{(1)}(t)}{dt} - 0.00575793Y^{(1)}(t) = 47.8204758X^{(1)}(t) + 36.486036$	1.3032

4. Control structure

Dynamic construction of the grey model uses only actual data, which represents real-time information about the sintering process, not depends on historical data and will make it possible to obtain the prediction of the charge temperature before the strand end. If the predictive temperature of the charge in the last point does not reach the setpoint, then it is necessary to control the sintering process. The control can be carried out by changing the amount of fuel in the initial charge, the strand speed, and the pressure created in wind boxes. The change in the amount of fuel affects only the charge that has not yet been fed to the sinter, therefore this effect is not considered in the current study.

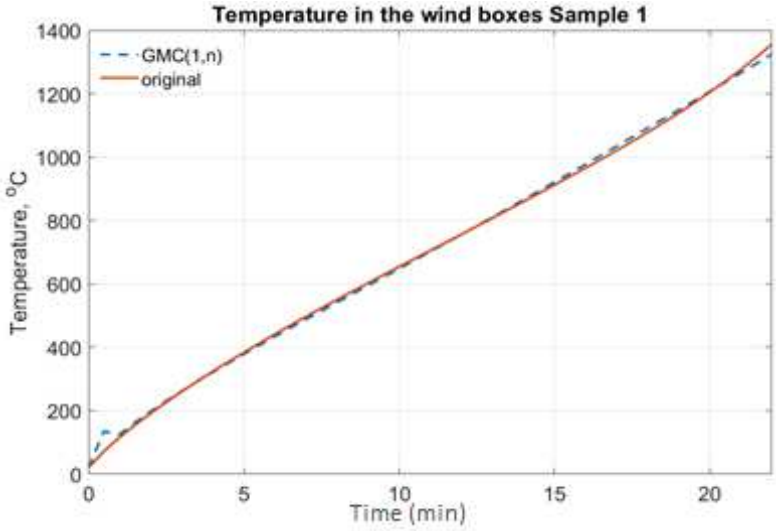

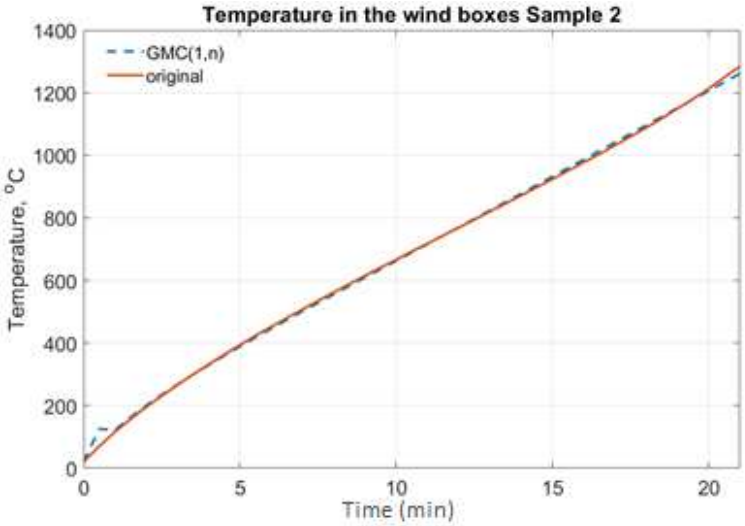

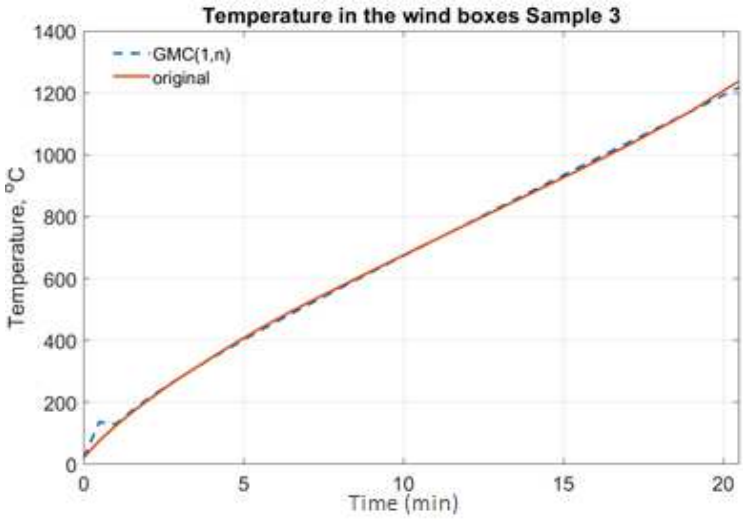

Figure 6 Predictive results for the samples

The proposed control structure for BTP is presented in Figure 7 and includes (1) data acquisition of temperature and pressure in wind boxes from the beginning of the process to a certain point, (2) construction of the grey predictive model GMC(1,n) based on the accumulated data, (3) prediction of the temperature up to the strand end, (4) optimization of process control parameters (speed and pressure in wind boxes) to achieve the desired temperature at the end of the process, (5) change of control parameters for the considered batch to obtain a good sinter quality and minimum return. The control structure is working in real-time and has the following algorithm: after the charge is passed under the horn, the system begins collecting data on temperature, pressure in the wind boxes and sinter machine speed. Based on the collected data, a forecast model is built on the basis of the grey model that predicts the temperature at the end of the sintering machine. If the temperature does not correspond to the BTP, a predictive optimization algorithm calculates the necessary values of the sinter speed and pressure in the wind boxes. The resulting values are fed to the appropriate controllers. After charge is reaching the end of sintering machine, the cycle is repeated for the next charge.

The particle swarm is used [25] as a method of predictive optimization. The particle swarm algorithm is a system of particles that move to optimal solutions, and each particle contains the coordinates of the found best solution (*pbest*) and the best solution from all the particles in the swarm (*gbest*). The following formula determines the direction and length of the particle velocity vector

$$\vartheta_i = \vartheta_i + a_1.rnd(\ ).(pbest_i - x_i) + a_2.rnd(\ ).(gbest_i - x_i) \tag{12}$$

where ϑ is particle speed vector, a_1, a_2 are constant accelerations and x is the particle's current position. Particle current position includes two variables: number of samples that represents time of sinter process and gas velocity.

As a criterion of optimality, the difference between the desired and predicted temperatures at the end of the sinter strand is used as follows

$$\left|\hat{Y}^{(0)}(t) - Y_{set_point}\right| \to \min \tag{13}$$

subject to

$$t_{\min} \le t \le t_{\max} \quad ; \quad X_{\min} \le X \le X_{\max}$$

where $\hat{Y}^{(0)}(t)$ is determined according to (9), the time step t is fixed to 0.5, and X is the pressure in the wind boxes.

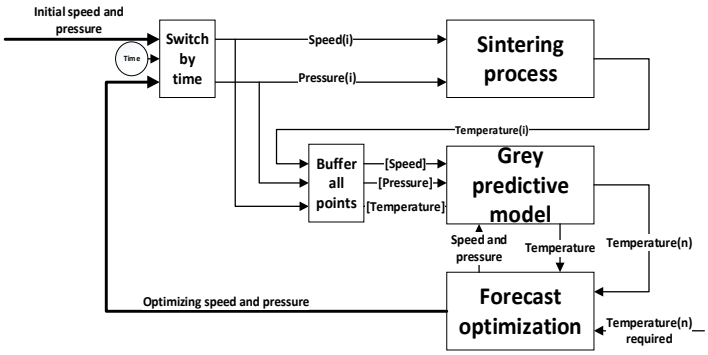

Figure 7 Control structure for BTP

With the help of the obtained optimal sintering process time t value, the strand speed is determined, and through the optimum gas velocity value, the pressure in wind boxes is found according to the Ergun Equation (1). Modeling results of BTP control system for the samples are represented in Figure 8 (data are provided in Appendix Table A2). In the first sample, the sintering temperature of the charge is reached in 22 minutes. To increase line productivity, extended boundaries of inequalities (13) are set. Wherein, the optimization algorithm allows us to find such values of strand speed and pressure in wind boxes at which the BTP is reached in 19.5 minutes. The sample 1 results of forecast optimization are as follows: the speed values change from 3.5 m/min to 4.5 m/min and the pressure in wind boxes from 800 mmHg to 760 mmHg. In the second sample, the BTP is not reached. Therefore, as a result of predictive optimization, a new value is supplied to the pressure regulator, at which the sintering temperature is reached. In the third case, as a result of predictive optimization, the speed of the sinter strand and pressure in wind boxes is increased, which allows us to achieve the optimum temperature in 19 minutes.

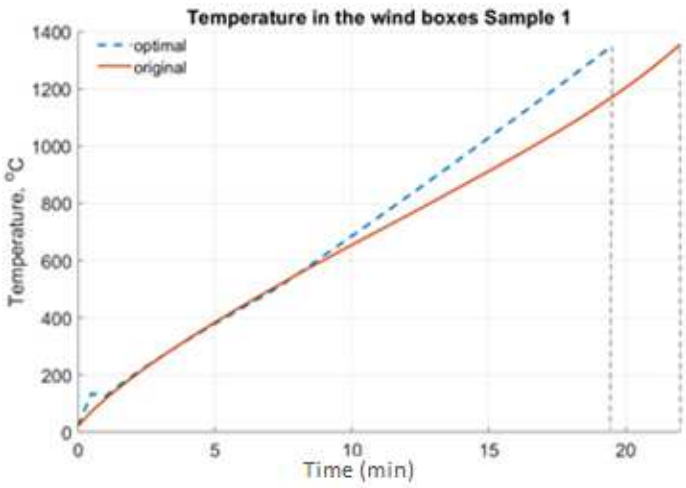

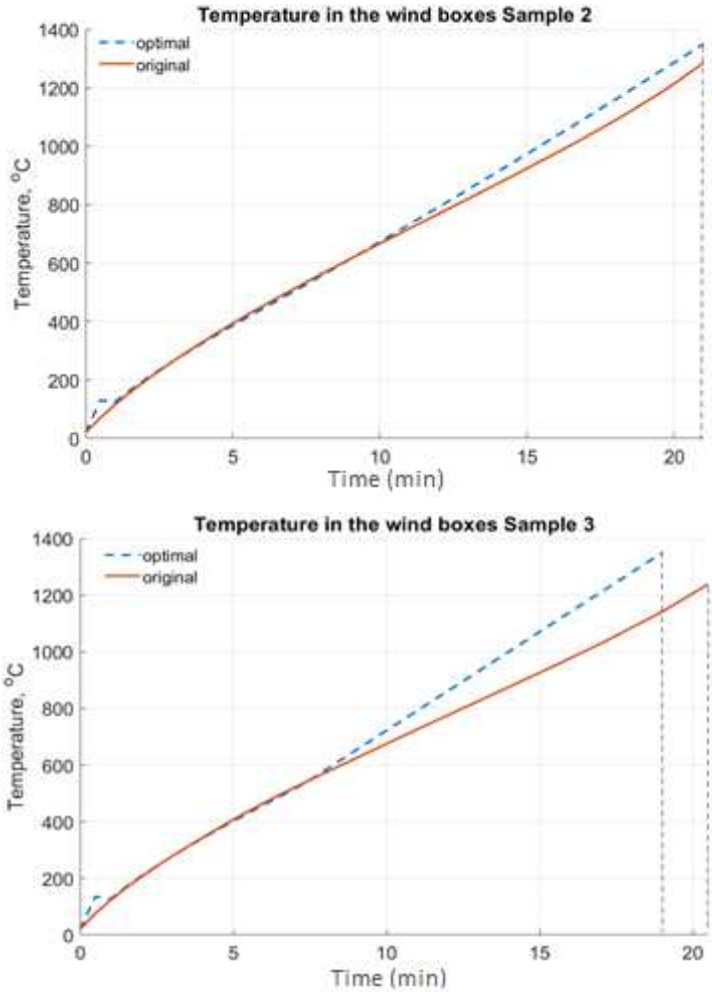

Figure 8 Control results of BTP for the three samples

5. Conclusion

The proposed control process structure of phosphorite ore sintering considered in this article is intended to improve the product quality and reduce the return. As an indicator responsible for the sintering quality, the BTP was chosen, i.e., the position at which the process reaches the highest temperature. Prediction of this variable was realized through the grey predictive model with some main contributions: (1) dynamic construction of the predictive model using small sample size, obtained from the beginning of the process, which reduces the time for data acquisition and system training; (2) control of the sintering process not only based on the strand speed, but also on the pressure in the wind boxes; (3) use of a grey model with (n-1) influencing factors that take into account not only the effect of the predicted value but also other process variables; (4) use of predictive optimization algorithm to determine optimal process parameters. In the current study's framework, the initial amount of data for constructing the model was also determined, as a result of which the amount of costs for building the data acquisition system is reduced, while the predictive model error

does not exceed 2%.

References

[1] Q. Feng, T. Li, X. Fan and T. Jiang. Adaptive prediction system of sintering through point based on self-organize artificial neural network. Trans. Nonferrous Met. Soc. China. 2000, 10(6):804-807.

[2] L. Peng, Z. Ji and J. Tan. Sintering finish point intelligent control. Proceedings of the 2005 IEEE/ASME International Conference on Advanced Intelligent Mechatronics Monterey, California, USA, 24-28 July, 2005.

[3] S. Du, M. Wu, X. Chen, X. Lai and W. Cao. Intelligent coordinating control between burn-through point and mixture bunker level in an iron ore sintering process. Journal of advanced Computational Intelligence and Intelligent Informatics. 2017, 21(1):140-147.

[4] M. Wu, C. Xu and Y. Du. Intelligent optimal control for lead-zinc sintering process state. Trans. Nonferrous Met. Soc, China. 2006, 16:975-981.

[5] M. Wu, C. Xu, J. She, and W. Cao. Neural-network-based integrated model for predicting burn-through point in lead-zinc sintering process. Journal of Process Control. 2012, 22:925-934.

[6] M. Wu, P. Duan, W. Cao, J. She and J. Xiang. An intelligent control system based on prediction of the burn-through point for the sintering process of an iron and steel plant. Expert Systems with Applications. 2012, 39(5):5971-5981.

[7] W. Cheng. An application of adaptive genetic-neural algorithm to sinter's BTP process. Proceedings of the Third Intemational Conference on Machine Learning and Cybernetics, Shanghai. 2004:3356-3360.

[8] W. Cheng. Prediction system of burning through point (BTP) based on adaptive pattern clustering and feature map. Proceedings of the Fifth International Conference on Machine Learning and Cybernetics, Dalian. 2006:3089-3094.

[9] X. Shang, J. Lu, Y. Sun, J. Liu and Y. Ying. Data-driven prediction of sintering burn-through point based on novel genetic programming. Journal of iron and steel research, International. 2010, 17(12):1-10.

[10] D. Wang, K. Yang, Z. He, Y. Yuan and J. Zhang. Application Research Based on GA-FWA in Prediction of Sintering Burning Through Point. Proceedings of 2018 International Conference on Computer, Communications and Mechatronics Engineering. 2018: 378-385.

[11] W. H. Kwon, Y. H. Kim, S. J. Lee and K. Paek. Event-based modeling and control for the burnthrough point in sintering processes. IEEE Transactions On Control Systems Technology. 1999, 7(1):31-41.

[12] J. Terpak, L. Dorcak, I. Kostial and L. Pivka. Control of burn-through point for agglomeration belt. Metalurgia. 2005, 44(4):281-284.

[13] C. Wang and M. Wu. Hierarchical intelligent control system and its application to the sintering process. IEEE Transactions On Industrial Informatics. 2013, 9(1):190-196.

[14] M. Wu, C.Wang, W. Cao, X. Lai, X. Chen. Design and application of generalized predictive control strategy with closed-loop identification for burn-through point in sintering process. Control Engineering Practice. 2012, 20:1065-1074.

[15] J. Shi, Y. Wu, L. Liao, X. Yan, J. Zeng and R. Yang. Soft sensing of the burning through point in iron-making process. Proceedings of 2016 IEEE 15th International Conference on Cognitive Informatics and Cognitive Computing, ICCI*CC. 2016.

[16] J. Deng. Introduction to grey system theory. The Journal of Grey System. 1989, 1:1-24.

[17] T. L. Tien. The indirect measurement of tensile strength of material by the grey prediction model GMC(1,n), Measurement Science Technology. 2005, 16:1322–1328.

[18] Y. Kaymak, T. Hauck, and M. Hillers. Iron ore sintering process model to study local permeability control. Proceedings of the 2017 COMSOL Conference in Rotterdam. 2017.

[19] T. Tien. A research on the grey prediction model GM(1,n). Applied Mathematics and Computation. 2012, 218:4903-4916.

[20] T. Tien. The indirect measurement of tensile strength for a higher temperature by the new model IGDMC(1,n). Measurement. 2008, 41:662-675.

[21] T. Tien. The indirect measurement of tensile strength by the new model FGMC (1,n). Measurement. 2011, 44:1884-1897.

[22] T. Tien. The deterministic grey dynamic model with convolution integral DGDMC(1,n). Applied Mathematical Modelling. 2009, 33:3498-3510.

[23] J. Kennedy and R. Eberhart. Particle Swarm Optimization. IEEE. 1995.

[24] A. M. Abdulshahed, A. P. Longstaff, and S. Fletcher. A cuckoo search optimization-based Grey prediction model for thermal error compensation on CNC machine tools. Grey Systems: Theory and Application. 2017, 7:146-1551.

[25] L. Wu and Z. Zhang. Grey multivariable convolution model with new information priority accumulation. Applied Mathematical Modelling. 2018, 62:595–604.

[26] S.A. Javed and S. Liu. Bidirectional Absolute GRA/GIA model for Uncertain Systems: Application in Project Management. IEEE Access. 2019, 1–9.

Appendix

Table A Erreur ! Document principal seulement. Initial data of temperature (y) and gas velocity (x)

Sample 1		Sample 2		Sample 3	
y	***x***	***y***	***x***	***y***	***x***
20,178	0,075294	20,18	0,075294	20,182	20,182
72,871	0,88249	70,2555	0,88621	76,4095	76,4095
115,63	0,7697	115,8425	0,76921	123,2425	123,2425
154,85	0,69239	157,1175	0,689593	166,2325	166,2325
191,66	0,63848	195,23	0,63322	205,2588	205,2588
226,68	0,59935	231,1367	0,594301	242,5869	242,5869
260,29	0,57933	265,8522	0,57159	278,4093	278,4093
292,71	0,55951	299,4536	0,552759	311,2645	311,2645
323,98	0,54366	331,8084	0,536016	343,988	343,988
354,19	0,53055	363,2904	0,522892	376,2741	376,2741
383,57	0,51914	393,986	0,511528	407,4144	407,4144
412,64	0,5096	423,6874	0,501888	437,4323	437,4323
441,21	0,50188	452,0936	0,49378	466,3269	466,3269
469,27	0,49504	480,0988	0,486933	494,165	494,165
496,8	0,48864	507,7149	0,481427	520,8768	520,8768
523,85	0,48367	535,1048	0,476668	546,8515	546,8515
550,5	0,47973	562,0962	0,473162	572,814	572,814
576,8	0,47673	588,727	0,470229	598,5332	598,5332
602,81	0,47449	615,1193	0,467746	624,2198	624,2198
628,61	0,47258	641,0877	0,466575	649,7711	649,7711
654,23	0,47128	666,8797	0,465865	675,2334	675,2334
679,71	0,47065	692,5236	0,465543	700,5228	700,5228
705,12	0,47066	717,9754	0,465922	725,7122	725,7122
730,57	0,47138	743,4423	0,466528	750,8114	750,8114
756,07	0,47245	768,9313	0,467423	775,8321	775,8321
781,69	0,47345	794,4997	0,46817	825,8002	825,8002
807,46	0,47422	820,125	0,468876	850,7832	850,7832
833,38	0,47482	845,8457	0,469539	875,8218	875,8218
859,46	0,47535	871,8297	0,47001	900,8902	900,8902
885,72	0,47592	897,8915	0,470425	926,039	926,039
912,14	0,47645	923,9532	0,470841	951,5448	951,5448
938,78	0,47691	950,4829	0,471147	977,4765	977,4765
965,68	0,47727	1004,016	0,471649	1003,408	1003,408
992,8	0,47756	1031,678	0,471833	1029,34	1029,34
1020,6	0,47781	1060,057	0,471965	1057,033	1057,033
1049	0,47801	1088,435	0,472097	1085,093	1085,093
1077,9	0,47815	1118,096	0,472182	1113,152	1113,152
1107,9	0,47826	1149,338	0,472207	1142,033	1142,033
1138,8	0,47832	1180,58	0,472233	1174,2	1174,2
1170,8	0,47836	1213,368	0,472249	1206,366	1206,366
1204,4	0,4784	1249,156	0,472246	1238,533	1238,533
1239,3	0,47844	1284,943	0,472242	-	-
1276	0,47846	-	-	-	-
1315	0,47849	-	-	-	-
1355,8	0,4785	-	-	-	-

Table A2 Simulation $\left(Y^{(0)}\right)$ and forecast data of temperature (y)

Sample 1		Sample 2		Sample 3	
$Y^{(0)}$	$\hat{Y}^{(0)}$	$Y^{(0)}$	$\hat{Y}^{(0)}$	$Y^{(0)}$	$\hat{Y}^{(0)}$
20,178	20,178	20,18	20,18	20,182	20,182
70,61841	135,1026	67,90837	130,5574	73,54634	135,7069
116,0574	125,1421	116,003	125,0854	123,7109	127,7107
156,3934	163,1588	158,421	164,5974	167,7012	170,1072
193,2281	197,9532	196,9186	200,6212	207,4161	208,4796
227,5997	230,4934	232,6748	234,2326	244,1281	244,0405

260,4307	261,6403	266,6648	266,3231	278,7166	277,6283
292,2474	291,8851	299,4707	297,4247	311,9073	309,9354
323,1613	321,3311	331,2649	327,6936	344,0714	341,3152
353,3544	350,1476	362,2125	357,2792	375,2855	371,8396
382,9465	378,4461	392,4691	386,3228	405,7092	401,6598
412,0341	406,3163	422,1354	414,9155	435,4849	430,9111
440,7172	433,8512	451,3054	443,1428	464,6882	459,665
469,0687	461,1188	480,06	471,0781	493,3748	487,9737
497,124	488,1521	508,4744	498,7897	521,6362	515,9242
524,9338	518,1465	536,609	527,064	549,5941	547,2869
552,5647	551,2897	564,5217	556,0531	577,3055	582,2083
580,0704	584,5612	592,2653	585,1531	604,7992	617,1279
607,4972	617,9613	619,8694	614,3646	632,1095	652,0455
634,8748	651,4907	647,3851	643,6879	659,2731	686,9613
662,2287	685,1499	674,8637	673,1235	686,3329	721,8751
689,594	718,9392	702,33	702,6718	713,3251	756,7871
717,0067	752,8593	729,8155	732,3333	740,2892	791,6972
744,5038	786,9106	757,3471	762,1083	767,2548	826,6053
772,1145	821,0937	784,9398	791,9973	794,2283	861,5116
799,8469	855,409	812,5979	822,0008	821,2167	896,416
827,693	889,857	840,3158	852,1191	848,2115	931,3184
855,6421	924,4384	868,0912	882,3528	875,1881	966,219
883,6878	959,1535	895,9172	912,7022	902,1438	1001,118
911,8296	994,003	923,7868	943,1678	929,0748	1036,014
940,0678	1028,987	951,6982	973,75	955,9771	1070,909
968,3994	1064,107	979,6485	1004,449	982,8485	1105,802
996,8201	1099,362	1007,64	1035,266	1009,688	1140,693
1025,325	1134,754	1035,669	1066,201	1036,495	1175,583
1053,913	1170,283	1063,726	1097,255	1063,265	1210,47
1082,579	1205,95	1091,808	1128,427	1089,991	1245,355
1111,323	1241,754	1119,914	1159,718	1116,672	1280,239
1140,14	1277,697	1148,042	1191,13	1143,308	1315,12
1169,031	1313,779	1176,189	1222,661	1169,896	1350
1197,992	1350	1204,355	1254,314	1196,435	-
1227,023	-	1232,539	1286,087	1222,924	-
1256,124	-	1260,741	1317,983	-	-
1285,296	-	-	1350	-	-
1314,538	-	-	-	-	-
1343,849	-	-	-	-	-